IEEE

Sensors Letters

MARCH 2018 VOLUME 2 NUMBER 1 ISLECD (ISSN 2475-1472)

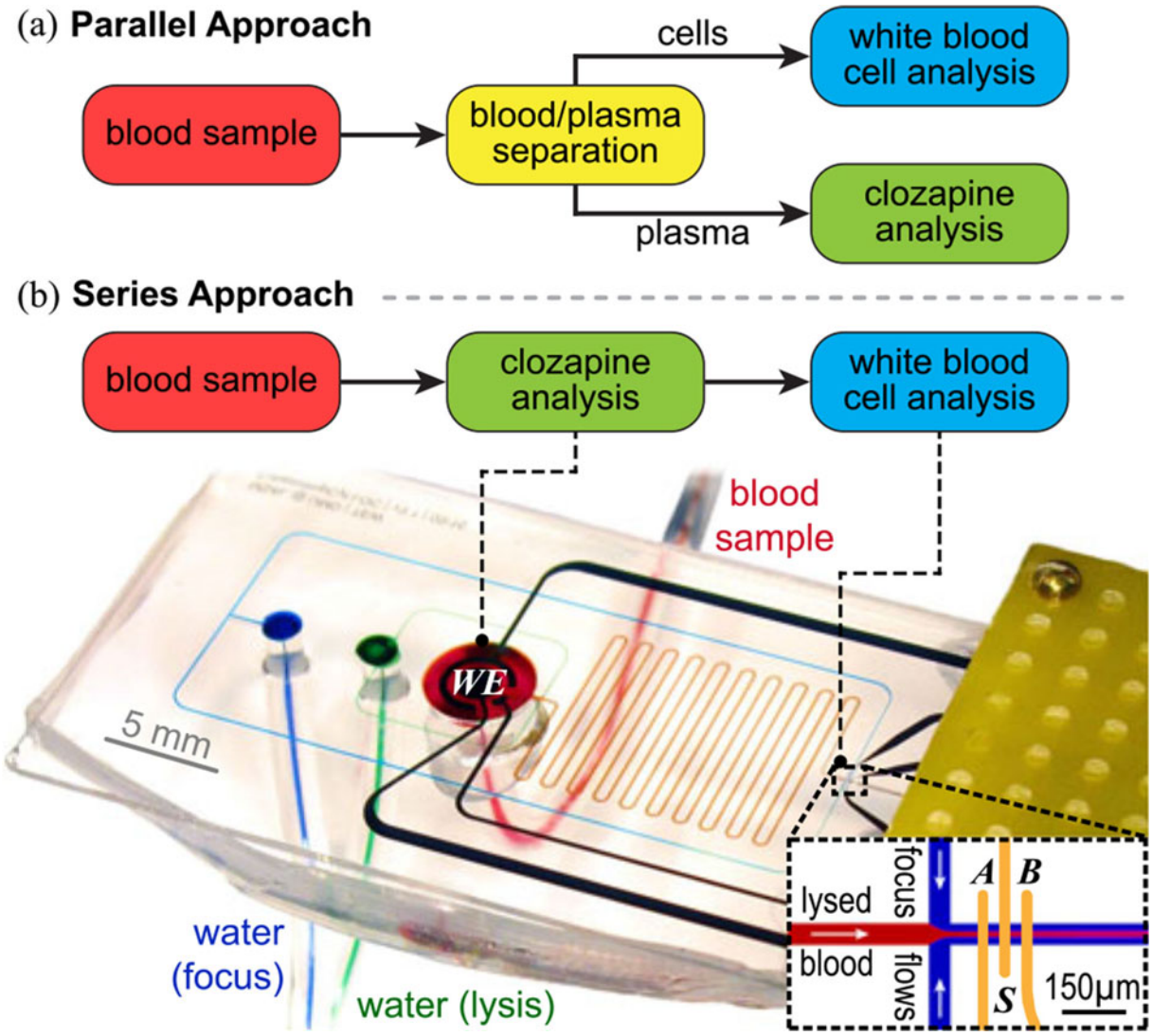

IEEE Sensors Council

A PUBLICATION OF THE IEEE SENSORS COUNCIL
www.ieee.org/sensors

IEEE

Sensor systems

The Role of Microsystems Integration Towards Point-of-Care Clozapine Treatment Monitoring in Schizophrenia

Thomas E. Winkler[1,2,5*], Florence O. Stevenson[1,2], Eunkyoung Kim[3], Mijeong Kang[3], Gregory F. Payne[2,3], Deanna L. Kelly[4], and Reza Ghodssi[1,2**]

[1]*MEMS Sensors and Actuators Laboratory, Department of Electrical and Computer Engineering, Institute for Systems Research, University of Maryland, College Park, MD 20742 USA*
[2]*Fischell Department of Bioengineering, University of Maryland, College Park, MD 20742 USA*
[3]*Institute for Bioscience and Biotechnology Research, University of Maryland, College Park, MD 20742 USA*
[4]*Maryland Psychiatric Research Center, University of Maryland School of Medicine, Baltimore, MD 21228 USA*
[5]*Department of Micro and Nanosystems, KTH Royal Institute of Technology, Stockholm 100 44, Sweden*
**Member, IEEE*
***Fellow, IEEE*

Manuscript received October 6, 2017; revised December 5, 2017; accepted December 11, 2017. Date of publication December 13, 2017; date of current version December 29, 2017.

Abstract—We present a perspective on microsystems integration aspects for concurrent cellular and molecular sensing in a lab-on-a-chip device. While of interest for a range of applications, very few–narrowly focused–examples of such devices can be found in the literature. Here, we approach the challenge from a systems level, considering sensor integration both in parallel and in series. Our study is specifically geared toward schizophrenia treatment, where concurrent blood monitoring of the antipsychotic clozapine and white blood cells could lead to improved treatment outcomes. We evaluate the critical system components for either design, namely, plasma skimming (parallel) and in-blood clozapine detection (series). We find that plasma skimming is infeasible but, for the first time, demonstrate direct detection of clozapine in whole blood. With a corresponding series-integrated microsystem, we finally demonstrate downstream white blood cell analysis on the same samples using impedance cytometry. We, thus, present the first lab-on-a-chip device capable of label- and reagent-free concurrent sensing of cellular and molecular markers.

Index Terms—Sensor systems, microsystems integration, impedance cytometry, plasma skimming, clozapine, white blood cells.

I. INTRODUCTION

Lab-on-a-chip devices and biosensors have rapidly proliferated for analytes ranging from ions to whole cells [1]. Works spanning multiple size scales, however, are comparatively rare due to challenges in systems integration. Yet such concurrent sensing is of great interest for a number of applications from cancer diagnosis (circulating tumor cells and protein biomarkers) to clozapine treatment monitoring in schizophrenia.

Clozapine (CLZ) is the most effective second-line antipsychotic available but remains underutilized due to the burden associated with regular centralized-laboratory blood tests for the drug itself (ensuring efficacy and avoiding toxicity), as well as for white blood cell (WBC) counts (avoiding agranulocytosis, a potentially serious side effect) [2], [3]. While individual point-of-care-suitable sensors for CLZ in human serum [4], [5] and for WBC in clinical blood samples [1], [6] have previously been presented, an integrated system presents unique challenges. To the best of our knowledge, only one group has published on concurrent cellular and molecular biomarker sensing, geared toward the aforementioned cancer diagnostics application [7], [8]. Since it targets low-count cells and relies on labels, however, wider applicability remains limited.

Corresponding authors: T. E. Winkler and R. Ghodssi (e-mails: winklert@kth.se; ghodssi@umd.edu).
Associate Editor: S. Tadigadapa.
Digital Object Identifier 10.1109/LSENS.2017.2782883

Two broad strategies are available to achieve concurrent cellular (WBC) and molecular (CLZ) analysis as illustrated in Fig. 1: (a) copying typical laboratory procedures by applying blood/plasma separation to connect the WBC and CLZ sensing modalities in parallel; or (b) integration of both sensors in series, with the CLZ measurement conducted directly in whole blood. The latter approach yields a simpler and thus ultimately more robust microfluidic device; the former provides the CLZ sensor with a less complex matrix and thus potentially higher sensitivity. Here we explore both strategies for overcoming remaining integration challenges towards concurrent cellular and molecular sensing in whole blood. We first consider critical system components, and ultimately demonstrate a novel microsystem capable of concurrent CLZ and WBC analysis.

II. SYSTEM COMPONENTS AND DESIGN

CLZ detection: We employ a composite chitosan film (F) with carbon nanotubes (CNT) and graphene (GP) to facilitate redox catalysis. This electrochemical approach eliminates the need for labels or chemical separation. We have previously presented sub-clinical (<1 μM) limits of detection in serum samples from patients with both F-CNT [4] and F-GP [5], with the latter study also demonstrating excellent selectivity (zero false positives for non-CLZ subjects). Direct detection of CLZ in whole blood samples, however, has to date not been demonstrated and is critical for a series design.

WBC detection: We rely on dual-frequency impedance cytometry. This has previously been shown to enable differential analysis of

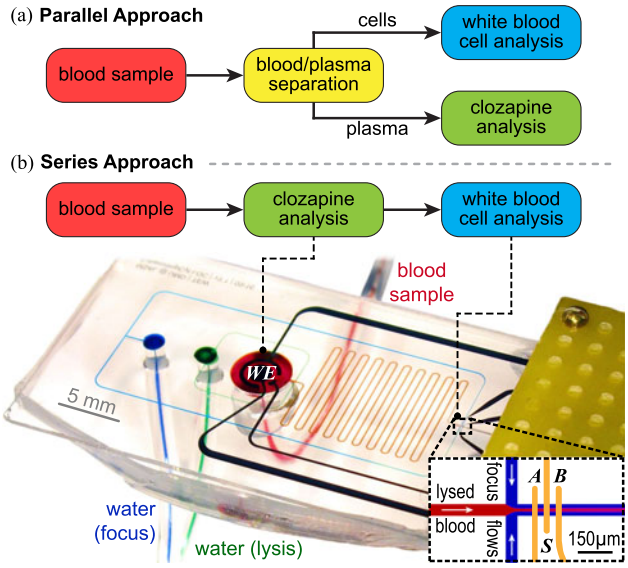

Fig. 1. Two strategies for integrating concurrent cellular and molecular analysis toward CLZ treatment monitoring. For the series approach, we include a photograph of our microsystem mounted in the experimental setup, with microfluidic flows highlighted by food coloring.

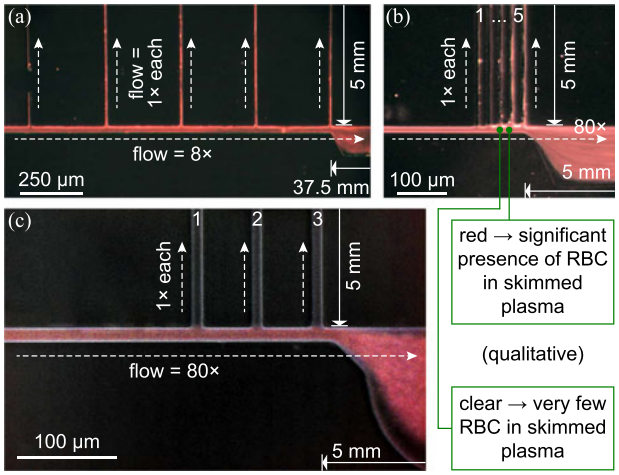

Fig. 2. Plasma skimming microscopy observations for exemplary designs with flow ratios of 8:1 (a) and 80:1 [(b) and (c)]. The blood inlet is on the left, and plasma skimming channels are toward the top. Optimized design (c) features enhanced corner definition and only three skimming channels.

WBC in clinical blood samples, and again does not rely on labels [6]. To further eliminate the need for chemical reagents in lysing the much more numerous red blood cells (RBC), we employ pure water for osmotic lysis [9], [10]. We additionally integrate hydrodynamic focusing to enhance sensitivity [11].

Blood/plasma separation: We select plasma skimming from the many available approaches [12]. It is the only method that promises i) continuous operation on ii) undiluted blood samples and that iii) does not rely on external forces. Although the underlying physics are complex, a simple design rule states that blood cells will exclusively follow one leg of a Y-junction given that its flow rate is at least 6× greater than that of the other leg [13]. This can be ensured through chaannel geometries that provide the correct fluidic resistance ratios. However, the principle has to date not been demonstrated with undiluted human blood, and is critical for a parallel design.

III. METHODS

Both the parallel and series approaches rely on i) 20 μm deep microfluidics with a width of 120 μm, except at the plasma skimming junctions (*cf.* Section IV-A) and the impedance cytometry electrodes (50 μm); and ii) gold electrodes for electrochemistry ($\varnothing = 2$ mm working (*WE*), equal-area concentric counter, and pseudo-reference) and impedance cytometry (*A, B, & S;* 25 μm width and gap). We define the electrodes in Au/Cr (200 nm/20 nm) on glass using a lift-off process. We cast the microfluidics in poly(dimethylsiloxane) and assemble devices following previously published procedures [14]. To render channel surfaces more hydrophilic, we treat them with 3% w/v Pluronic F-68. Finally, the composite F-CNT/GP is electrodeposited (90 s, 32 A/m² cathodic current) from solution (1% w/v each).

The resulting microsystem, mounted inside a custom Faraday cage, is illustrated for the series approach in Fig. 1(b). For impedance cytometry, we apply a sinusoidal voltage (90 kHz and 900 kHz; $V_{\max} < 1$ V; $V_{\text{offset}} = 0$) to electrode *S,* record the differential current $B-A$ using transimpedance- and lock-in amplifiers, and analyze the data using a wavelet-based adaptation of a published approach [15], [16]. CLZ analysis relies on differential pulse voltammetry (scanrate 2 mV/s; pulses 0.2 s, 50 mV).

Human whole blood (acid-citrate-dextrose anticoagulant) was obtained from a blood bank (Tennessee Blood Services) and used within 72 h of delivery. Immediately prior to experiments, blood is supplemented with 5 mM ethylenediaminetetraacetic acid, 3 μM ticagrelor, 10 μM tirofiban, and 100 U/ml streptokinase to inhibit platelet aggregation, and filtered through a 50 μm mesh (Filcon). Fluidics are actuated using infusion syringe pumps (New Era 1002X), connected *via* Tygon tubing, at a combined flowrate of 170 μl/h.

IV. RESULTS AND DISCUSSION

To assess the challenges associated with integrating the components into a single microsystem, we begin our study by focusing on plasma skimming (A) and whole-blood CLZ sensing (B). These are the components first encountered by the sample in the parallel and series cases, respectively (*cf.* Fig. 1) and, thus, serve as the critical link. Based on those findings, we subsequently implement and validate an integrated microsystem with WBC analysis (C).

A. Parallel Design—Plasma Skimming

To evaluate plasma skimming for its suitability in our microsystem, we fabricate >50 devices of various fluidics-validation designs with flow ratios from 8:1 to 110:1 at each of either three or five channel junctions. This is achieved by varying the blood outlet channel's fluidic resistance from high (120 μm wide, 37.5 mm long) to low (200 μm wide, 5 mm long) at a constant plasma channel geometry (10 μm wide, 5 mm long). We choose a consistent depth of 20 μm based on ease of prospective systems integration with impedance cytometry, where this is optimal in balancing WBC sensitivity with risk of clogging.

We show representative results from three designs in Fig. 2, featuring flow ratios of 8:1 (a) and 80:1 (b–c). Unlike for sheep blood [13]

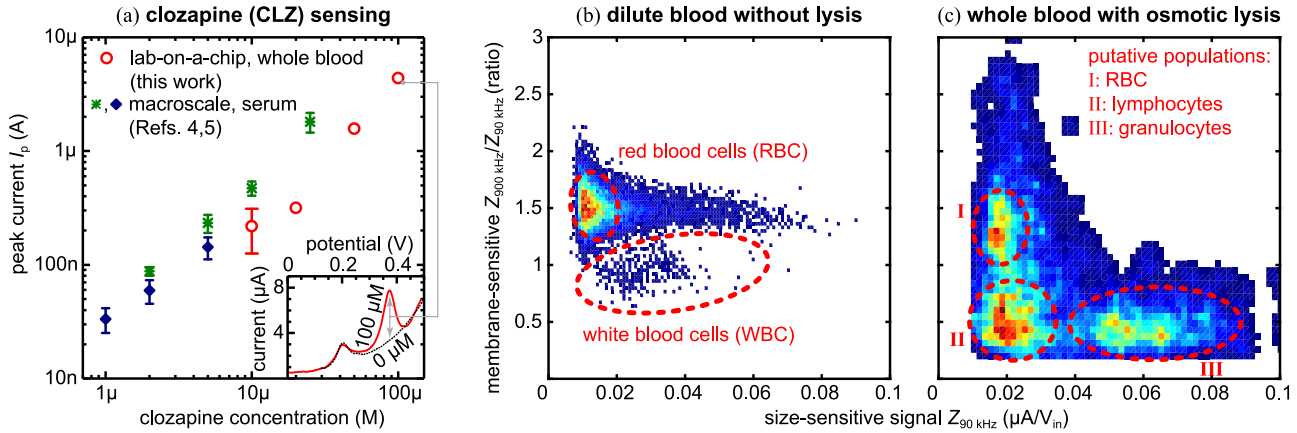

Fig. 3. (a) Electrochemical peak currents I_p for CLZ detection directly in whole blood with lab-on-a-chip (red; $N = 5$) compared to detection in serum at the macro-scale (green [4], blue [5]), indicating comparable sensitivity. Error bars (where available) represent the standard deviation. (Inset) Differential pulse voltammograms from human whole blood with (red) or without (black) 100 μM CLZ. (b), (c) Scatterplots/heatmaps (low to high counts: blue to red) of cellular impedance signals Z at 90 kHz (x-axis; size-sensitive) and 900 kHz (y-axis; membrane-sensitive; normalized for size-based effects), for 2000× diluted blood without lysis as a negative control (b; $N \sim 11\,000$) and undiluted whole blood with on-chip, reagent-free pure water lysis (c; $N \sim 1500$). Cell populations of note are outlined in red and showcase the differential blood cell analysis capabilities.

and 9× dilute human blood [17] as in previous studies, we witness significant penetration of RBC (red) into all of the thin side channels at 8:1 (a). Though we do not quantify separation efficiency, we can qualitatively confirm plasma skimming by channels appearing clear, observed only for flow ratios >50:1 (1–3 in Fig. 2(b) and (c)). Between the two 80:1 designs shown, we still note a marked difference in performance in spite of identical flow ratios. This arises out of two factors. First, the number of skimming channels: although this does not impact the flow at equilibrium, fewer junction points yield higher stability when the equilibrium is perturbed by cell aggregates [12]. Second, junction corner definition (b–5 μm resolution; c–1.5 μm): this likewise does not affect the hydrodynamic flow ratios; however, rounded corners will divert the RBC streamlines further into the plasma channels and allow cells to escape more easily due to inertial effects (4–5 in b), which we thus hypothesize play a non-negligible role. Even the optimized design from Fig. 2(c), however, remains prone to clogging in the constricted plasma skimming region–out of 12 test devices, over half failed within 5 min, and none remained operational past 15 min of use.

While this is sufficient for sensing *e.g.*, CLZ or protein markers [17] on the plasma component, it is not compatible with the continuous cellular flow requirement of a downstream WBC counter. An integrated parallel design would thus require a different blood/plasma separation approach. The available alternatives, however, would all raise new system-level integration challenges due to *e.g.*, relying on very high flow rates or different channel depths [12], thus impacting the overall microfluidic design.

B. Series Design—Whole Blood Clozapine Sensing

To evaluate F-CNT/GP sensing performance, we test 6 devices by flowing whole blood with CLZ (0, 10 [2×], 20, 50, or 100 μM) through their 5 mm diameter, ~250 μm deep detection chambers. We record a clear CLZ redox signal (red) at the expected 0.37 V on top of the intrinsic whole blood background (black) as exemplified in Fig. 3(a) (inset). The background closely resembles that previously observed in serum, with a peak around 0.2 V attributed to uric acid [4], [5].

We plot the measured peak currents I_p from our devices alongside those from macro-scale serum experiments (F-CNT [4] and F-GP [5]) in Fig. 3(a). From these, we can determine a sensitivity of 1.3 ± 0.2 (*vs.* 1.0 and 0.9) $\log(I_p)/\log[\text{CLZ}]$, showing that sensor performance is well conserved in spite of the more complex environment and smaller sample volumes in the present work. The limit of detection increases to 3.8 (*vs.* 0.8 and 0.5) μM. This is driven by two factors: First, signal magnitudes are reduced by ~50%. A large part of this can be attributed to CLZ partitioning into blood cells [18], meaning that 10 μM in whole blood actually corresponds to a serum measurement of ~7 μM. The remainder is likely due to blood cell crowding and film fouling restricting the diffusion of plasma CLZ. Second, between-device/sensor signal variability appears to increase by a factor of ~3. We attribute this to the F-CNT/GP coating process in the microsystem, which likely suffers from the inhomogeneous electric field due to variable positioning of the external wire counter electrode employed.

Although the detection limit falls at the upper end of the 1–3 μM (serum) clinical range [2], [3], it is sufficient to detect toxic levels of CLZ, and importantly establishes the feasibility of employing well-characterized CNT and/or GP-based CLZ sensing directly in whole blood at the microscale. We further expect that more homogenous electrodeposition using a fixed, planar counter electrode would reduce variability, and higher film carbon loading could amplify signals.

C. Integrated Microsystem

Both plasma skimming and whole blood CLZ sensing reveal limitations as discussed–alongside the strategies to address these–in the respective sections. The CLZ detection limit in whole blood, however, presents only a component-level optimization challenge for the series design, independent of the rest of the system and, thus, inherently more straightforward to address.

We thus proceed to implement a fully integrated device (only) for the series design as pictured in Fig. 1(b). Therein, the blood sample (red) first enters the CLZ detection chamber, and indeed the data in the previous Section were obtained in such devices. Immediately after the

chamber outlet, the blood is exposed to pure water (green) to initiate osmotic lysis of the RBC as flow continues through the serpentine channels. The sample is then focused hydrodynamically with another stream of water (blue) prior to passing over the impedance cytometry electrodes.

To validate this impedimetric WBC analysis, we initially show representative signals Z for a lysis-negative control (PBS instead of water) in Fig. 3(b). To avoid signal saturation, in this case only we dilute the whole blood by 2000×. The numerous RBC yield a readily apparent population in the scatterplot. The tail with constant membrane-sensitive signal of ∼1.5 is due to coincident detection of RBC, which cannot be avoided in spite of dilution. We note that the true number of RBC is expected to significantly exceed the population captured here due to only certain geometric orientations of the discoid cells yielding a large enough signal to pass our filter algorithm. The second feature of note is the small (∼250) but distinct population with membrane-sensitive signals of 1 or lower, corresponding to the–in this sample rare–WBC, which cannot be further differentiated.

In Fig. 3(c) we proceed to demonstrate the true concurrent cellular/molecular sensing capabilities in our integrated microsystem, showing data corresponding to downstream analysis of one of the undiluted whole blood samples in Fig. 3(a). With osmotic lysis, the scatterplot now reveals at least three distinct populations. The overall pattern here agrees well with that observed in previous studies with reagent-based lysis [6]. The membrane-sensitive signals >1 can be attributed to debris from lysis as well as to a small number of surviving (swollen) RBC. This is supported by comparison with (b) and the slight positive shift in size-sensitive signals. At membrane-sensitive signals <1, two WBC populations can now be identified: lymphocytes (∼40%), only slightly larger than RBC and thus with similar size-sensitive signals; and the much larger granulocytes (∼50%). The ratios here match expectations, particularly considering that we obtained the samples from a blood bank (rather than fresh), falling well within the respective reference ranges of 16–48% and 39–81% [19]. A positive shift in size-sensitive signals of the WBC populations with respect to (b) is again indicative of swelling on pure water exposure, which may aid differentiation between sub-populations. The WBC populations also exhibit a negative shift in membrane-sensitive signals compared to (b). This can be attributed to the change in solution conductivity due to osmotic lysis, to which the membrane-sensitive signals are more responsive.

V. CONCLUSION

We explored microsystems integration aspects for concurrent cellular and molecular sensing both in parallel and in series. We investigated plasma skimming as the critical component for parallel integration and found that long-term operation is infeasible with undiluted human blood. Toward series integration, we demonstrated for the first time the detection of clozapine directly in whole blood. We found that sensitivity is largely conserved compared to macro-scale serum studies, though future component optimization regarding particularly the detection limit is called for. Based on the evaluation of these critical components, we chose the series design for our fully integrated microdevice. In this, we further demonstrated downstream impedance cytometry for white blood cell analysis in the same blood sample. We thus showcased the first lab-on-a-chip concept for label- and reagent-free concurrent cellular and molecular analysis. Our integrated system represents an important step toward point-of-care monitoring for clozapine treatment in particular. More broadly, our systems integration study and the resulting device serve as a blueprint for other applications requiring analysis of targets spanning molecular to cellular size scales.

ACKNOWLEDGMENT

The authors would like to thank H. Ben-Yoav for useful discussions. This work was supported in part by the National Institutes of Health under Grant R56-MH105571, in part by the Robert W. Deutsch Foundation, and in part by the Maryland NanoCenter and its FabLab.

REFERENCES

[1] W. Jung, J. Han, J.-W. Choi, and C. H. Ahn, "Point-of-care testing (POCT) diagnostic systems using microfluidic lab-on-a-chip technologies," *Microelectron. Eng.*, vol. 132, pp. 46–57, 2015.

[2] R. W. Buchanan *et al.*, "The 2009 schizophrenia PORT psychopharmacological treatment recommendations and summary statements," *Schizophrenia Bull.*, vol. 36, pp. 71–93, 2010.

[3] D. L. Kelly *et al.*, "Blood draw barriers for treatment with clozapine and development of point-of-care monitoring device," *Clin. Schizophrenia Relat. Psychoses*, 2015, doi: 10.3371/CSRP.KEBE.070415

[4] E. Kim *et al.*, "Programmable 'Semismart' Sensor: Relevance to monitoring antipsychotics," *Adv. Funct. Mater.*, vol. 25, pp. 2156–2165, 2015.

[5] M. Kang *et al.*, "Reliable clinical serum analysis with reusable electrochemical sensor: Toward point-of-care measurement of the antipsychotic medication clozapine," *Biosens. Bioelectron.*, vol. 95, pp. 55–59, 2017.

[6] X. Han, C. van Berkel, J. Gwyer, L. Capretto, and H. Morgan, "Microfluidic lysis of human blood for leukocyte analysis using single cell impedance cytometry," *Anal. Chem.*, vol. 84, pp. 1070–1075, 2012.

[7] W. Huang, "Concurrent detection of cellular and molecular cancer markers using an immunomagnetic flow system," *Anal. Chem.*, vol. 87, pp. 10205–10212, 2015.

[8] W. Huang, "Separation and dual detection of prostate cancer cells and protein biomarkers using a microchip device," *Lab. Chip*, vol. 17, pp. 415–428, 2017.

[9] P. Sethu, "Microfluidic isolation of leukocytes from whole blood for phenotype and gene expression analysis," *Anal. Chem.*, vol. 78, pp. 5453–5461, 2006.

[10] T. E. Winkler, H. Ben-Yoav, D. L. Kelly, and R. Ghodssi, "Osmotic erythrocyte lysis for chemical- and label-free impedance cytometry," in *Proc. IEEE Int. Conf. Solid-State Sens., Actuators, Microsyst.*, Anchorage, AK, USA, 2015, pp. 351–354.

[11] T. E. Winkler, H. Ben-Yoav, and R Ghodssi, "Hydrodynamic focusing for microfluidic impedance cytometry: A system integration study," *Microfluid. Nanofluidics*, vol. 20, 2016, Art. no. 134.

[12] S. Tripathi, Y. V. B. V. Kumar, A. Prabhakar, S. S. Joshi, and A. Agrawal, "Passive blood plasma separation at the microscale: A review of design principles and microdevices," *J. Micromech. Microeng.*, vol. 25, 2015, Art. no. 083001.

[13] S. Yang, A. Ündar, and J. D. Zahn, "A microfluidic device for continuous, real time blood plasma separation," *Lab. Chip*, vol. 6, pp. 871–880, 2006.

[14] M. T. Meyer *et al.*, "Multi-depth valved microfluidics for biofilm segmentation," *J. Micromech. Microeng.*, vol. 25, 2015, Art. no. 095003.

[15] M. Evander, A. J. Ricco, J. Morser, G. T. A. Kovacs, L. L. K. Leung, and L. Giovangrandi, "Microfluidic impedance cytometer for platelet analysis," *Lab. Chip*, vol. 13, pp. 722–729, 2013.

[16] F. Caselli and P. Bisegna, "A simple and robust event-detection algorithm for single-cell impedance cytometry," *IEEE Trans. Biomed. Eng.*, vol. 63, no. 2, pp. 415–422, Feb. 2016.

[17] R. Fan, "Integrated barcode chips for rapid, multiplexed analysis of proteins in microliter quantities of blood," *Nat. Biotechnol.*, vol. 26, pp. 1373–1378, 2008.

[18] R. Flanagan, B. Yusufi, and T. Barnes, "Comparability of whole-blood and plasma clozapine and norclozapine concentrations," *Br. J. Clin. Pharmacol.*, vol. 56, pp. 135–138, 2003.

[19] National Center for Health Statistics, "Complete blood count," 2017.